Neural Network Based Fractional Order PID Controller for Harmonic Mitigation of Induction Motor Drive System

1st Workagegn Tatek Asfu
Department of Electrical and Computer Engineering
Debre Berhan University
Debre Berhan, Ethiopia
workagegntatek@gmail.com

2nd Solomon Feleke Aklilu (PhD)
Department of Electrical and Computer Engineering
Debre Berhan University
Debre Berhan, Ethiopia
sole12@dbu.edu.et

3rd Daniel Abebe Beyene
Department of Electrical and Computer Engineering
Debre Berhan University
Debre Berhan, Ethiopia
abebe.daniel7@gmail.com

***Abstract*—Torque produced in IM (induction Motor) is collected fundamental torque, however, due to core saturation, air gap irregularity, and winding distribution; stator and rotor slotting harmonics torque are produced. This reduces the quality of the power system, life span, and performance of the motor and the controller device. In this paper, a neural network, based fractional order proportional integral derivative (NNFOPID) controller is designed to compensate the harmonics of the induction motor driving system. FOPID controller parameters have been tuned automatically based on the delta-learning rule with sigmoid activation function. The active shunt capacitor is directly connected to five- level three-phase inverter directly controlled by sinusoidal pulse width modulation (SPWM). Based on the reference and measured harmonics, error the controller parameter of FOPID is tuned using NN (neural network) delta learning algorithm. The design of discrete type PI speed and current vector controller is followed by space vector pulse width modulation (SVPWM) is deigned to track the actual speed of IM to the reference speed. The IM modeling and power electronics driving the system within its harmonics effect was analyzed and discussed. In addition, the effect of current and voltage harmonics with different conditions is illustrated. For this NNFOPID controller parameter a tuning was designed and Matlab simulations check the system performance. The result shows that the current harmonic and voltage harmonic were reduced to 2.79%, 12.12%, respectively.**

***Index Terms*—Neural network, Fractional order PID, Vector control, five level three phase inverter**

I. Introduction

Introduction motors are chosen for various industrial applications mainly due to low manufacturing and material costs. Due to nonlinear loads in industry motors, drives and other power electronics devices are the source of harmonics. This reduces the quality of the power system and increases the hysteresis and eddy current loss of the motor. Different researches were conducted on how to improve the performance and to mitigate harmonics of square cage induction motors.

In [1], the harmonics of hub type five-phase induction motor with different winding approaches for electric traction drive system were studied. In the study, the finite element method was used to the mathematical modeling of five-phase IM and the effect of harmonics was analyzed. When the load increase the harmonics increases, and the lesser harmonic generated in the concentric topology compared to other winding topologies. The author in [2], illustrated the mitigation of harmonics for IM based on injection and passive filter method, in which it was concluded the injection method has better performance than passive filter one. Paper in [3], discussing the comparison of different pulse generation, closed and open loop control with SVPWM pulse generation for IM drive system with the effect of load on tracking ability was the main question. The result shows that as the load increase, the tracking ability decreases.

In [4], to mitigate the effect of current harmonics on the induction motors drive, FOPID control was designed. To determine the control parameter, a phase margin rule was used and the result was explained with the comparison of the convectional PID controller. The learning adaptability of phase margin is not dynamic compared to artificial neural network. The authors in [5], proposed that the use of feed-forward neural network to estimate the speed of IM and field-oriented vector control was used as a control technique and this has reduced the cost of sensor and the effect of aging. The estimated and measured results shows oscillatory to high frequency noises, which generate harmonics on the system. The author [6] has used a stator current- based model reference adaptive control to estimate the speed of the induction motor and compensate the disturbance due to parameter variation.

The review on induction motor modeling, control, and parameter estimation is reviewed in [7]. In [8], the total harmonics analysis of an induction motor using a five-level inverter is presented, and as a level in the inverter's construction increases, the harmonic distortion is minimized. In most power systems, harmonics are generated due to

non-linear loads and solid-state drive systems, as discussed in [9]. Development of multistage power electronics drives and nonlinear control strategies solves this problem. To address the problem of set-point tracking and effect of harmonics, the mathematical modeling of the IM and all effects of internal and external disturbances on the system was analyzed. To improve the system performance and regulation, system modeling and design of fractional order PID control and neural network based parameter tuning were used. To mitigate the effect of harmonics on the system, five-level three-phase inverter designed. SVPWM is used to control the two-level three-phase inverter operations. After the modeling of a system and controller design as well as control parameter tuning MATLAB Simulink simulation was done.

This paper concentrated on providing guidelines of artificial neural network such as dynamical parameter tuning for fractional order PID control parameter and for stability and robustness analysis of the IM drive systems.

II. Harmonics Modeling and Field Oriented Control of Three Phase Induction Motor

This paper presents a field oriented control of three phase IM based on mathematical transformations of the standard three-phase induction motor model into specific two phase d-q coordinate model and the effect of harmonic on the motor and power transmission line. The general proposed system modeling block diagram is shown in Fig 1. In [10], the authors introduce the steady-state mathematical model based on vector space decomposition and symmetrical components theory. At first, finite element analysis is used to investigate different air gap flux harmonics and different harmonic current components induced in the cage rotor circuit, and with this five-star connection, improved fault tolerance is achieved when compared to a conventionally star-connected stator.

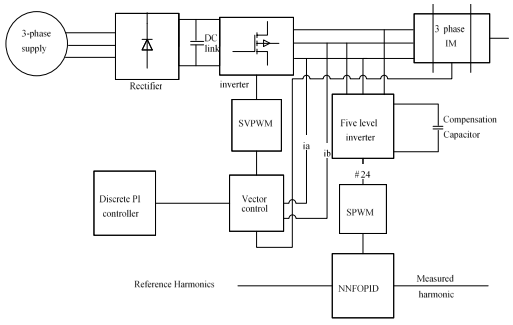

Fig. 1: General Block diagram of the proposed system

A. Mathematical modeling of the induction motor and Effects of harmonics

The authors in [11] studied the detection of harmonics in renewable energy resources such as wind and the reduction of total harmonic distortions for dynamic loading conditions using an active power filter based on an ADALINE neural network. In the work, the design was also trained by a back propagation algorithm in which the load, current, and voltage will be analyzed.

In [12], mathematical modeling of a squirrel cage three-phase induction motor using second Kirchhoff's laws with Maxwell's equation is developed. The authors proposed in [13], phase voltages harmonics mitigation of induction motor drive system using series active filters. The stator winding is feed from the primary voltage source inverter and the secondary voltage source inverter which is controlled to cancel the harmonics.

The harmonic generated in the industry is due to a variable speed driving system (power electronics devices), a load that varies with impedance and from IM. The torque produced in IM is collected through fundamental torque, however, due to core saturation, air gap irregularity, winding distribution, stator and rotor slotting harmonic torque are produced. Harmonics torque due to winding distribution, stator and rotor slot is high compared to air gap irregularity and core distribution harmonic. The distribution factor is defined as$k_d = \frac{\sin\left(\frac{\gamma}{2}\right)}{min\left(\frac{\gamma}{2}\right)}$, where $m\gamma = a$ phase spread, $m = a$ number of lines per phase, γ=slot angle for induction machine, the spread is 120^0. $k_d = \frac{\sin\left(\frac{n\gamma}{2}\right)}{min\left(\frac{n\gamma}{2}\right)}$, n is the order of harmonics.

If $k_{dn} = 0$, n^{th} harmonics are eliminated, $k_{d3} = 0$, $k_{d9} = 0$,$k_{d15} = 0$, when $m\gamma = 120^0$ then the triple harmonics are eliminated. The remaining harmonics are 5^{th}, 7^{th}, 11^{th}, 13^{th}, 17^{th}, and so on. The existing harmonic has been derived using the relation $6m - 1$ and $6m + 1$ that is shown in Table I. The general expression of Fourier series harmonic

TABLE I: Order of generated harmonic in IM

m	6m-1	6m+1
1	5	7
2	11	13
3	17	19

magnetic flux of IM is expressed as

$$f_r = \frac{3}{2} f_m \cos(\theta - \omega t) + \frac{3}{2} f_m \cos(\frac{\theta}{2} - \frac{\omega}{2} t) + \frac{3}{2} f_m \cos(\theta - \frac{\omega}{7} t) + \cdots \quad (1)$$

Mathematical modeling of three-phase IM with mechanical faults is presented in [14]. The author consider the effect of saturation and nonlinearity of the magnetic core. The fundamental equivalent circuit of an IM per phase equivalent and harmonic equivalent circuit are shown in Fig. 2 and Fig. 3 respectively. For analysis and controlling purpose, the two-phase winding modeling is simpler than the three phase winding modeling. The equivalence modeling of two phase and three phase windings are shown in Fig.4.
The mathematical relation of three-phase to two-phase wind-

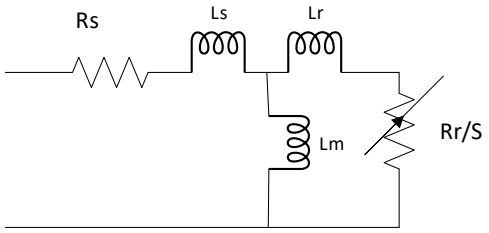

Fig. 2: Per-phase equivalent circuit of induction motor

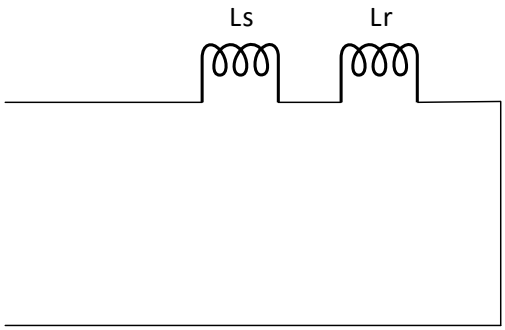

Fig. 3: Three harmonic equivalent circuit

ings in the stationary frame are presented in Equations (2) and (3) as follows

$$i_\alpha = i_a \cos(0^0) + i_b \cos(120^0) + i_c \cos(240^0) \quad (2)$$
$$i_\beta = i_a \sin(0^0) + i_b \sin(120^0) + i_c \sin(240^0) \quad (3)$$

The three phase fundamental voltages are

$$V_{aN-1} = V_m \sin \omega t \quad (4)$$
$$V_{bN-1} = V_m \sin \omega t - 120^0 \quad (5)$$
$$V_{cN-1} = V_m \sin \omega t + 120^0 \quad (6)$$

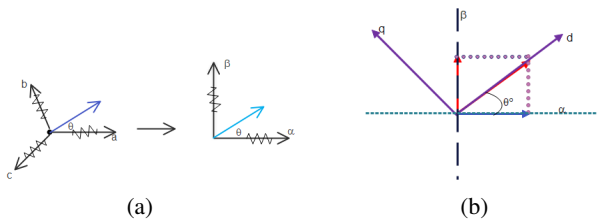

(a) (b)

Fig. 4: Equivalent modeling of three-phase induction motor in different reference frame

The three phase fundamental flux can be expressed in terms of the stator voltage, this relation is as follows

$$V_{aN-1} = i_{a-1} R_s + \frac{d\psi_{a-1}}{dt} \quad (7)$$
$$V_{bN-1} = i_{b-1} R_s + \frac{d\psi_{b-1}}{dt} \quad (8)$$
$$V_{cN-1} = i_{c-1} R_s + \frac{d\psi_{c-1}}{dt} \quad (9)$$

Mathematically the three phase n^{th} harmonics voltage is described in equations

$$V_{aN-1} = V_{m-n} \sin(n(\omega t)) \quad (10)$$
$$V_{bN-1} = V_{m-n} \sin(n(\omega t - 120^0)) \quad (11)$$
$$V_{cN-1} = V_{m-n} \sin(n(\omega t + 120^0)) \quad (12)$$

From equation (10)-(12) the harmonic voltage and revolving magnetic field 5^{th}, 11^{th}, 15^{th} and the order like this, the phase sequence is reversed and produces a magnetic field revolving in the opposite direction. The harmonic voltage 3^{rd}, 7^{th}, 13^{th} and the order like this has same phase sequence with the fundamental voltage. The revolving magnetic field is also the same direction with fundamental voltage. Revolving magnetic fields to fundamental, fifth and seventh harmonics as shown in Fig 5.

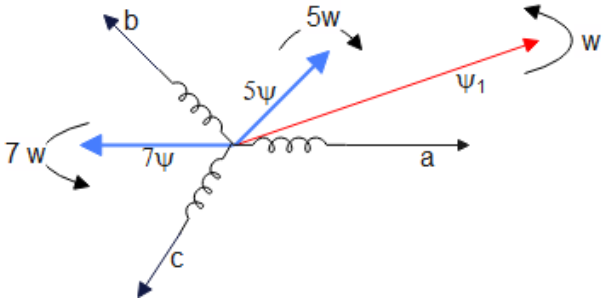

Fig. 5: Relation between fundamental flux and harmonics

B. *Frequency of stator and rotor magnetic fields*

Applied stator voltage contains fundamental and harmonics such as fifth, seventh, 11th, 13th and higher order harmonics, and the stator magnetic fields revolving at ω,-5ω, 7ω,-11ω, -13ω. The magnetic motive force and rotor magnetic field waves move with respect to the rotor frequency of $(\omega - \omega_r)$,$(-5\omega - \omega_r)$,$(7\omega - \omega_r)$,$(-11\omega - \omega_r)$,$(13\omega - \omega_r)$.

The intersection of the fundamental flux with harmonic current and the intersection between the fundamental current with harmonic flux produce a pulsating torque. An interaction between the fundamental flux with the fifth and seventh harmonic current produce a sixth harmonic torque. In a similar way, due to the interaction of fundamental flux with higher order harmonics, the produced order of harmonic torque is 12, 18, and 24.

III. Field Oriented Controller Design

In field-oriented control (FOC), the principle of decoupled torque and flux control are applied and it relies on the instantaneous control of stator current space vectors. Control of IM is complicated due to the control of decoupled torque and flux producing components of the stator phase currents. In [15] , induction motor modeling and vector control with a variable PID gain controller algorithm have been presented. There is no direct access to the rotor quantities such as rotor flux and current. To overcome these difficulties, a high performance vector control algorithms are developed which can decouple the stator phase currents by using only the measured stator current, flux and rotor speed. In this paper, indirect field oriented control (IFOC) is selected due to its performance. In [16], to regulate the torque and current of an IM an adaptive control loop is designed and flux estimation technique is used. In [17], the speed control of three-phase IM using indirect field oriented control using direct axis current control based on PID controller is discussed.

In [18] this paper discussed indirect field oriented control (IFOC) based on PID control used speed control of 3-phase induction motor. However, this work parameter variation and speed estimation technique was not included.

The authors in [19], investigate the design of an optimal fractional order PID controller experimentally to stabilize the effect of the current and harmonics on the induction motors due to imbalance current, and as compared to the conventional PID controller, the performance of the proposed controller is better in terms of harmonic current, vibration, and noise reduction.

In [20] , the velocity, the stator current, and the developed thrust of a three-phase linear induction motor were improved by using a recurrent wavelet neural network with a PID controller. Moreover, the particle swarm optimization is employed to tune the parameters of the proposed controller, and with the proposed controller, rising time, steady state error, overshoot, and settling time are improved over the conventional wavelet neural network. PID based speed controller with numerical tuning is used to observe the transient speed performance of IM and validated by real-time control through the real-time workshop (RTW) in MATLAB Simulink then integrated with three-phase voltage source inverter (VSI) is presented in [21].

In [22], mathematical modeling of three-phase induction motor using two-phase stationary reference frame in dq axis is analyzed and simulation model using Matlab has been discussed.

In indirect field orientation, the synchronous speed is the same as the instantaneous speed of the rotor flux vector and the d-axis of the d-q coordinate system is exactly with locked on the rotor flux vector (rotor flux vector orientation). Indirect field oriented control; here the rotor flux angle is measured indirectly, instead of using air gap flux sensors. IFOC estimates the rotor flux by computing the slip speed (ω_{sl}). The stationary d and q axes fixed on the stator and the rotor d and q axes fixed on the rotor flux.

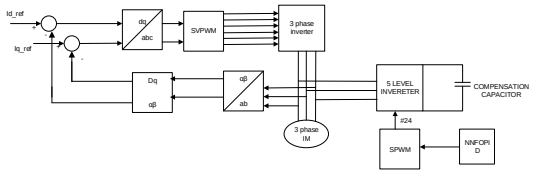

Fig. 6: General Block diagram of the proposed system

A. Discrete PI Vector controller design

A linear diagonal control strategy of stator current-based field-oriented control used for three-phase induction motors is presented in [23]. A separate phase control of a single input, single output discrete type controller for induction motors has been discussed in [24]. The authors in [25], proposed self-tuning PID controller based on backpropagation artificial neural network for speed response improvement of direct current motor.The discrete mathematical function of PI controller is design based on Euler backward and trapezoidal approximation rule.

$$u(k) = k_p e(k) + k_i \left[\frac{T_s}{2}[e(k) + 2e(k-1) + e(k-2)] + previuos_{int} \right] \tag{13}$$

In discrete time the PI controller has two zeros plus one pole at the unit circle. Based on the discrete model of the plant and controller, the speed and current controller of IM is presented in equation (14)and (15).

$$G_{C-current}(z) = \frac{k_p + k_i T_s (1 - e^{-nT_s})}{\sigma L_s n} \times \left(\frac{1}{z - 1 + \frac{k_p + k_i T_s (1 - e^{-nT_s})}{\sigma L_s n}} \right) \tag{14}$$

where $n = \frac{R_s}{\sigma L_s} + \frac{L_m^2}{\sigma L_s L_r T_r}$, $T_r = \frac{L_r}{R_r}$ and $\sigma = 1 - \frac{L_m^2}{L_s L_r}$.

Closed loop transfer function of the speed controller with the system is obtained as

$$G_{C-speed}(z) = \frac{k_p + k_i T_s (1 - e^{-mT_s})}{\beta} \frac{1}{k} \times \left(\frac{1}{z - 1 + \frac{k_p + k_i T_s (1 - e^{-mT_s})}{\beta} \frac{1}{k}} \right) \tag{15}$$

where $k = \frac{3}{4} \frac{L_m}{L_r} p \psi_{dr}$, $m = \frac{\beta}{J}$, β and J are coefficient of friction and momentum of inertia respectively.

The unknown parameter of the PI controller parameter

has been tuned using system tracking criteria. The tuning criterion is based on the close loop transfer function of the system. For the tracking purpose, it is desired to have the following requirement:-

$$\frac{\omega_{rm}}{\omega_{rm-error}} = 1 \quad \forall |G_c G_p| > 1 \tag{16}$$

1) The required gain for the crossover frequency is $|G(j\omega_c g)G(j\omega_c g)| = 0dB$
2) Specified phase margin ψ_m represented as $-\pi + \psi_m = arg(G(j\omega_c g)G(j\omega_c g))$
3) Robustness against variation of against of the plant, so around the gain cross over frequency phase of the open loop transfer function must be constant. $\frac{d}{d\omega}\left(arg(G(j\omega_c g)G(j\omega_c g))\right) = 0$ at $\omega = \omega_c g$
4) For reducing the high frequency noise at high frequencies of closed loop transfer function must have small magnitude. $G(j\omega) = \frac{G_c(j\omega)G_p(j\omega)}{1+G_c(j\omega)G_p(j\omega)} \leq AdB$ at frequency of $\omega = \omega_c$
5) The sensitivity function must have small magnitude at low frequencies. To reduce and track the reference it should have satisfied the following condition.

$$S(j\omega) = \left|\frac{1}{1 + G_c(j\omega)G_p(j\omega)}\right| \leq BdB$$

at frequencies $\omega = \omega_c$

B. Space vector pulse width modulation

As shown in Fig. 6 Two-phase voltage and the stator reference frame are transformed to three-phase stator reference, and which acts as the modulating voltage for the modulator that uses the state space pulse width modulation (SVPWM) scheme. The modulator output which is in the form of pulses are used to drive the IGBT with antiparallel diodes acting as switches for the conventional two-level three-phase voltage source inverter (VSI).

To minimize the switching loss that is caused by the pure SVPWM, Max-Min offset is added to the inject third harmonics and reduce the requirement of filter design. In this respect max-min SVPWM is used. Based on [26], the design of the offset is presented as follows:

$$Offset = -\left(\frac{V_{max} + V_{max}}{2}\right)$$
$$V_{max} = max\{V_{an}, V_{bn}, V_{cn}\}$$
$$V_{min} = V_{min\{V_{an}, V_{bn}, V_{cn}\}}$$

The output voltage magnitude reaches the same value as that of the third harmonics injection PWM. The principle of SVPWM requires the determination of a sector, calculation of vector segments, and it involves region identification based on the modulation index and calculation of switching time duration's. The two level, three-phase inverter drive IM contributes to harmonics generation. To reduce this multilevel inverter is designed to control the harmonics in the source side as well as in the load side.

C. Five Level three-phase Inverter design

Five level diode clamped multilevel inverter fed induction motor drive has been designed based on the voltage level active switches, clamping diodes, and DC capacitors.The design specification is shown in Table II.

TABLE II: Order of generated harmonic in IM

Voltage level(V)	Active switches 6(V-1)	Clamping diodes3(V-1)(V-2)	DC capacitor (V-1)
5	24	36	4

The three-phase five-level inverter, it has three similar construction legs. The switching sequence of one leg is presented in Fig. 7.

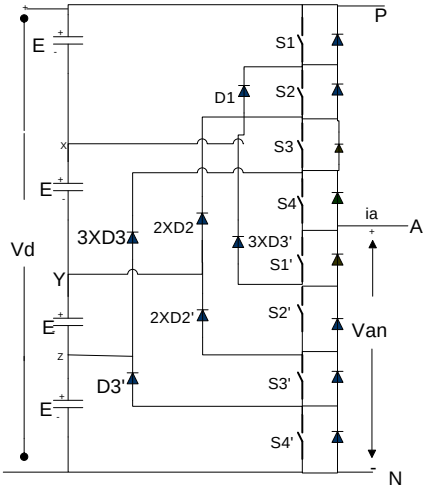

Fig. 7: Circuit diagram of one leg five-level inverter

Three-phase five level inverter used to mitigate the harmonics on the transmission line and IM drive system as it is shown in the Fig. 7. The others two legs, legs for phase B and phase C are similar with phase A which is shown in Fig. 7.

TABLE III: Switch sequence of five level inverter for one leg

S_1	S_2	S_3	S_4	$S_1^{'}$	$S_2^{'}$	$S_3^{'}$	$S_4^{'}$	V_{an}
1	1	1	1	0	0	0	0	4V
0	1	1	1	1	0	0	0	3V
0	0	1	1	1	1	0	0	2V
0	0	0	1	1	1	1	0	1V
0	0	0	0	1	1	1	1	0V

IV. Fractional order PID Controller design

From the theory of fractional calculus we have

$$aD_t^{\alpha} = \begin{cases} \frac{a^{\alpha}}{dt^{\alpha}}\ nc/m^3 & R(\alpha) > 0 \\ 1 & R(\alpha) = 0 \\ \int_{\alpha}^{t}(dt)^{-\alpha} & R(\alpha) < 0 \end{cases} \tag{17}$$

Where a, and t, are limit of operation, D is the fundamental differential operator, α is order of operation, $R(\alpha)$ real part of α.

The discrete mathematical modeling of FOPID is illustrated in Equation (20). Based on the Rieman Lioville fractional calculus definition the fractional order PID controller is formulated as:

$$G_c(s,p) = k_p + \frac{k_i}{s^\lambda} + K_d s^\sigma \tag{18}$$

To discretized the linear controller changing the S domain in to Z domain; using the relation

$$S^{\pm r} = \left(\frac{2}{T}\frac{1-z^{-1}}{1+z^{-1}}\right)^{\pm r} \tag{19}$$

Using Equation (2) and (3), we can get the fractional PID controller as follows

$$G(z) = k_p + \frac{k_i}{\left(\frac{2}{T}\right)^\lambda \left(\frac{1-z^{-1}}{1+z^{-1}}\right)^\lambda} + k_d \left(\left(\frac{2}{T}\right)^\lambda \left(\frac{1-z^{-1}}{1+z^{-1}}\right)^\sigma\right) \tag{20}$$

To tune the parameters of the controller, extended delta learning rule is used.

A. Extended Delta Learning method

The neural network is capable of generalizing and learning the dynamic relationships between the input and output of system. It is a mathematical model and provides the nonlinear relationship between the system input and output. The neural networks can constantly update their connection weights to respond to changes in the plant dynamics. It constantly update their connection weights to respond to changes in the plant dynamics. Extended delta rule learning method feature of the neural networks can be exploited in auto-tuning the FOPID gains. The structure of neural network used in this paper consists of three main inputs, and five outputs and two hidden layers. The values of controller gain parameters of the FOPID were tuned due to continuously updating weights and biases of the neural network. The unknown parameter of the fractional order PID controller parameter has been tuned using the extended delta learning rule. In this study, the harmonic mitigation of the induction motor is controlled by the NNFOPID. The Neural Network tuned is controlled via FOPID gain parameters optimal selection. As shown in Fig. 8, the optimal solution obtained via neural Network control FOPID gain value. The delta rule changes the weights of the neural connections to minimize the difference between the net input to the output, y_{in}, and the target value td. The aim is to minimize error over all training patterns. However, this is accomplished by reducing the error for each pattern, one at a time. Accumulate weight corrections can be also over a number of training patterns if desired.
Parameters of FOPID controller are adapted while running neural FOPID tuner learner system, without a priori model. Mathematical modeling of extended delta neural network algorithm can be derived as follows.

The neural network architecture for the proposed model

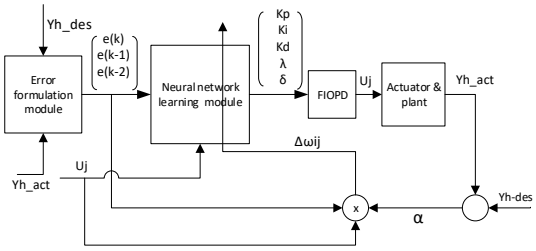

Fig. 8: Block diagram of NNFOPID controller tuning

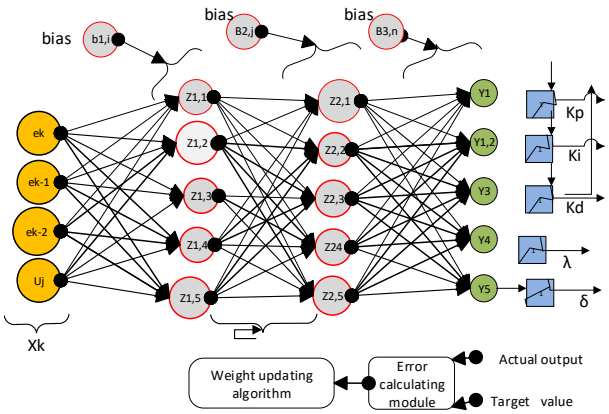

Fig. 9: Neural network archtecture of the systemBlock diagram of NNFOPID controller tuning

to tune FOPID controller parameter is shown in the Fig. 9
Based on the Fig. 9, the mathematical derivation of the net input to the hidden and output layer can be expressed as follows:

$$Z_{1,i} = \Sigma_{i=1}\Sigma_{k=1}(x_k W_{ki})\vec{e} + b_{1,i} \tag{21}$$

The unit vector representation of the first hidden layer is shown in equation (2)

$$Z_{1,i} = Z_{1,1}\vec{e}_1 + Z_{1,2}\vec{e}_2 + Z_{1,3}\vec{e}_3 + Z_{1,4}\vec{e}_4 + Z_{1,5}\vec{e}_5 + b_{1,i} \tag{22}$$

The second hidden layer written as

$$Z_{2,i} = \Sigma_{j=1}\Sigma_{i=1}(Z_{1,i}W_{ji})\vec{e}_j + b_{2,i} \tag{23}$$

$$Z_{2,i} = Z_{2,1}\vec{e}_1^{'} + Z_{2,2}\vec{e}_2^{'} + Z_{2,3}\vec{e}_3^{'} + Z_{2,4}\vec{e}_4^{'} + Z_{2,5}\vec{e}_5^{'} + b_{2,i} \tag{24}$$

$$y_{1,n} = \Sigma_{n=1}\Sigma_{j=1}(Z_{n,j}W_{jn})\vec{e}_n + b_{3,n} \tag{25}$$

$$y_{1,n} = y_{1,1}\vec{e}_1^{''} + y_{1,2}\vec{e}_2^{''} + y_{1,3}\vec{e}_3^{''} + y_{1,4}\vec{e}_4^{''} + y_{1,5}\vec{e}_5^{''} + b_{3,n} \tag{26}$$

The output of the sigmoid function is defined as:

$$y_{ink} = f(y_{1,n}) \tag{27}$$

The weight that is needed to be adjusted with respect to a new data point, to minimize the objective function is the minimized form of the mean square error. Let the cost function J and the target value is t_l.

$$J = \frac{1}{2}\Sigma_i\Sigma_n(t_{1,n} - y_{ink,l})^2 \tag{28}$$

Minimization via steepest descent with optimization step and by using the activation function for the output layer is sigmoid, then the updated control parameter

$$O_k = \frac{1}{1 + e^{-\gamma_{ink}}} \tag{29}$$

$$\Delta_{n,l} = -\alpha\frac{\partial J}{\partial W_{n,l}} = -\alpha\left(\frac{\partial J}{\partial y_{ink}}, \frac{y_{ink}}{\partial Z_{2,j}}, \frac{\partial Z_{2,j}}{\partial Z_{1,i}}, \frac{\partial Z_{1,i}}{\partial w_{k,i}}\right) \tag{30}$$

For the sigmoid activation function

$$\Delta w_{n,l} = -\alpha(t_l - y_{ink})t_l(1 - y_{ink})x_k \tag{31}$$

The gradient the error function become,

$$\begin{aligned}\frac{\partial J}{\partial W_{n,l}} &= \frac{\partial}{\partial w_{n,l}}\left(\Sigma_k(t_{l,n} - O_k)^2\right) \\ &= -(t_k - O_k)f(y_{ink,l})\frac{\partial}{\partial w_{n,i}}(y_{ink}) \\ &= (t_k - O_k)\left(\frac{\partial}{\partial w_{n,l}}f(y_{ink,l})\right)Z_{2,j}\end{aligned} \tag{32}$$

Letting $\sigma = -(t_k - O_k)\left(\frac{\partial}{\partial w_{n,l}}f(y_{ink,l})\right)$ the weight of the connection with the hidden layer until $Z_{2,j}$,

$$\frac{\partial J}{\partial w_{n,l}^{(1)}} = -\Sigma_k\frac{\partial}{\partial w_{n,l}^{(3)}}y_{ink,l} \tag{33}$$

Weight updating for the output and hidden layer is defined in Equation (34)-(36).

$$\Delta w_{n,l}^{(out)} = -\alpha\frac{\partial J}{\partial w_{nl}} = \alpha\sigma_k Z_{2,j} \tag{34}$$

$$\Delta w_{j,i}^{(2)} = -\alpha\frac{\partial J}{\partial w_{nl}} = \alpha\sigma_k Z_{1,i} \tag{35}$$

$$\Delta w_{k,i}^{(1)} = -\alpha\frac{\partial J}{\partial w_{nl}} = \alpha\sigma_k x_i \tag{36}$$

The loss optimization of the network weights that achieve the lowest error is expressed as follows, letting $w^* = argmin\left(\frac{1}{5}\sum_{i=1}^{5}L\left(f\left(X^{(i)};W\right),Y^{(i)}\right)\right)$ it is the same as the minimum of the gradient of the cost function

$$w^* = argmin\left(J(W)\right) \tag{37}$$

where $W = \left\{w_{j,i}^{(1)}, w_{j,k}^{(2)}\right\}$

B. Algorithm for Updating the Weight to Minimized the Error

1) Initialize weights randomly $\sim N(0, \sigma^2)$
2) Loop until convergence
3) Specified input of the data points, n
4) Compute gradient, $\frac{\partial J(W)}{\partial W} = \frac{1}{n}\sum_k^n\frac{\sigma J_k(W)}{\sigma W}$ this is used to be fast to compute and best estimate for the gradient
5) Update weight, $W_{update} = W - \eta\frac{\partial J(w)}{\partial W}$
6) Return weights

V. Results and Discussion

To initiate the training process, arbitrary values for the FOPID gain parameters could be assigned and be used as initial values. Then the FOPID parameters are modified and adjusted through online learning NN algorithm.

Based on the above-mentioned discussions, a max Min space vector space PWM was constructed with the PI controller that can be regulated to detect the harmonic current effect, speed control overshoot at steady state, and parameter variation of the IM performance is analyzed.

This study presents a three-phase IM whose harmonic effect and load variation can be reduced by using the NNFOPID controller design. The appropriateness of the parameter considering the IM and the effect of harmonic is verified by Matlab Simulation results. Fig.11 shows that Matlab simulation result of three phase current with two-level three-phase PID based vector control of induction motor for measuring the measured phase current waveform under the rated current $20A$. As shown in Fig. 10, the rotating speed commands between 0 and 1450 rpm are designed by the five level vector control method, and the optimal NNFOPID controllers were considered.

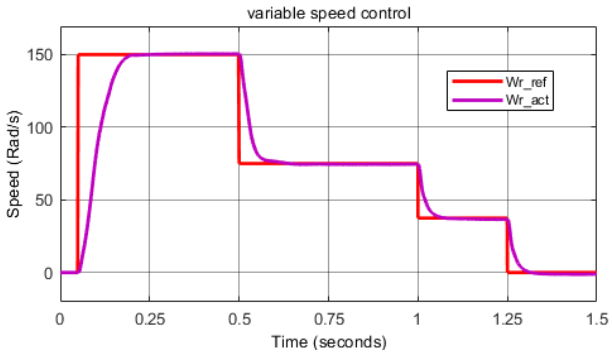

Fig. 10: Variable speed control of Induction motor

As shown in Fig 11. The current waveform is not smooth; it is distorted at the pick point. The harmonic level of this current wave form is discussed in Fig.12.

The simulation result of two level three-phase inverter with SVPWM IM drive is shown in Fig. 12. As a result, the total harmonic detection is 69.84% and the dominant harmonic is the third level harmonic, which is around 32.45%. The

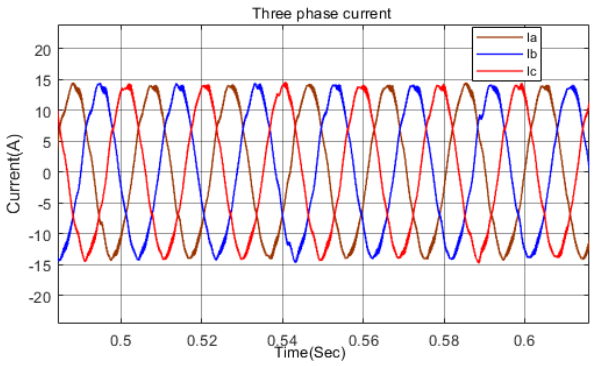

Fig. 11: Three phase current with two level Max Min space vector control technique

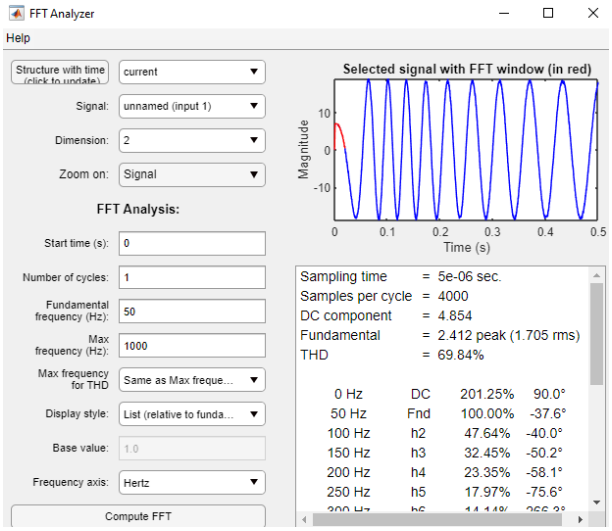

Fig. 12: Current harmonics when two level three-phase inverter with rated load torque 45N

harmonics decreases for higher order level.

The current harmonics were compensated using the five-level three-phase inverter with NNFOPID vector control technique. At the full load, the harmonic level of current and voltage is shown in Fig. 13.

As shown in Fig. 13, shows that the list of current harmonics in the form of bar type fast Fourier transform analysis and with relative to the fundamental frequency analysis. The total harmonic detection reduced to 2.79%. The dominant harmonic is the third with 1.35%. In Fig. 15, at no load condition the current harmonic increased to 5.5%. The motor is loaded with 50% of the rated value, current harmonic mitigation improved to 2.82%. As shown in Fig. 14 and Fig. 15, the motor run without load could generate more harmonics than loaded up to its rated value. The NNFOPID based vector control of IM drive improved the harmonic generated due to nonlinear loads and parameters of the motor. The effect of voltage harmonic in IM is compared with two

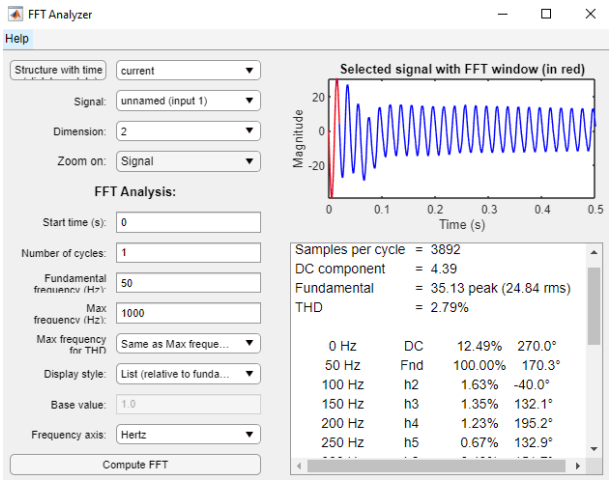

(a)

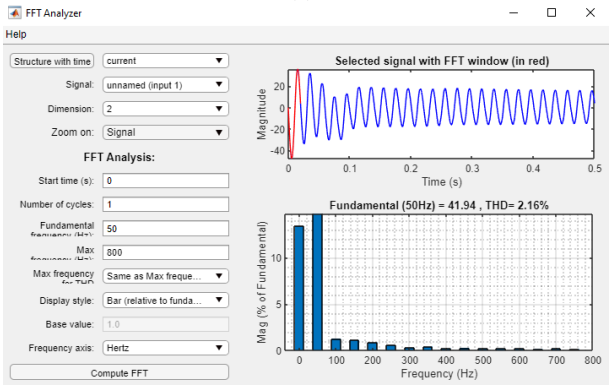

(b)

Fig. 13: Current harmonics when a five level inverter with NNFOPID and load torque 45N

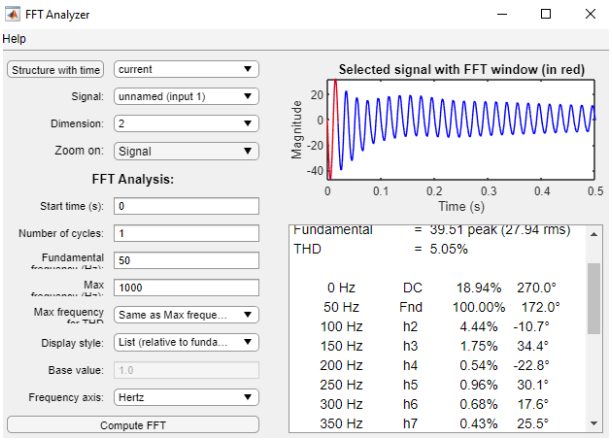

Fig. 14: Harmonics currents with five level inverter and NNFOPID with no load condition

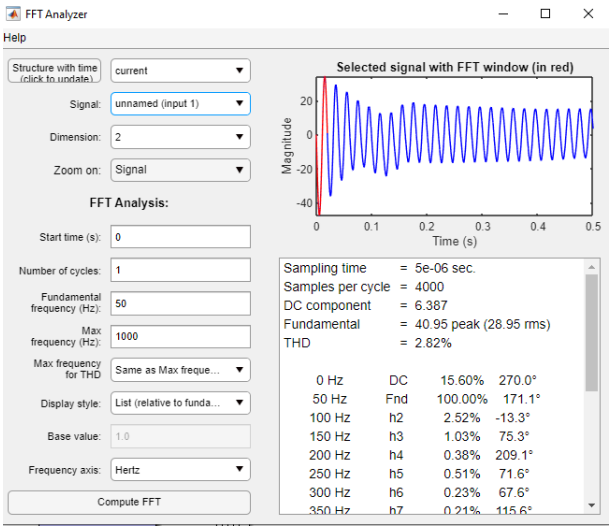

Fig. 15: Harmonics voltage with five level inverter and NN-FOPID with 25N load torque

level three phase inverter derived by PID vector controlled and five-level three-phase inverter controlled by SPWM with NNFOPID controller is compared with full rated torque, 50% of the rated torque and no load condition.

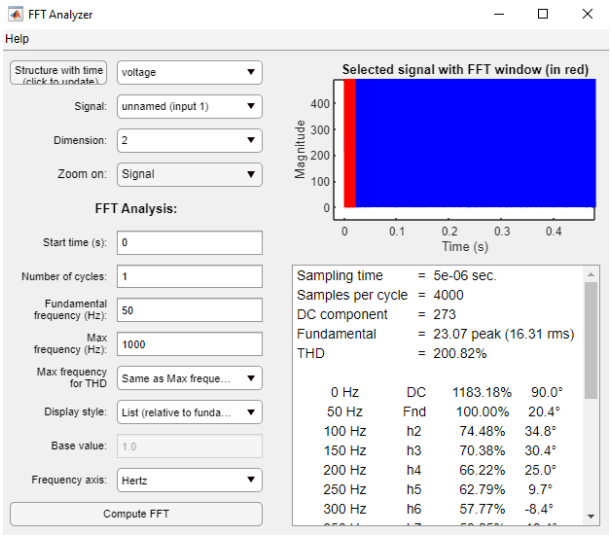

Fig. 16: Harmonics voltage with two level three-phase inverter with load torque 45N

From the above Fig. 16, the total harmonic detection is 200.82% and the dominant harmonic is the third level harmonic, it is around 70.38%. The voltage total harmonic detection is high and it will disturb the power system, in addition, it will increase the billing cost and reduce the life span of the motor. The NNFOPID improved voltage harmonic is shown in Fig. 17. With full rated torque and rated speed, the total harmonic detection of the system is 12.12%.
No-load conduction of five-level three-phase inverter with NNFOPID control of IM controller the total harmonic Matlab

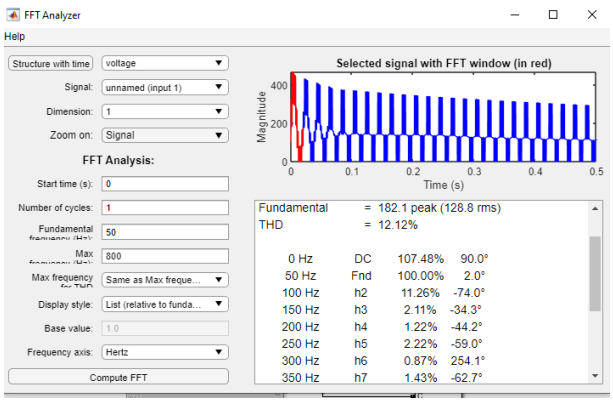

(a)

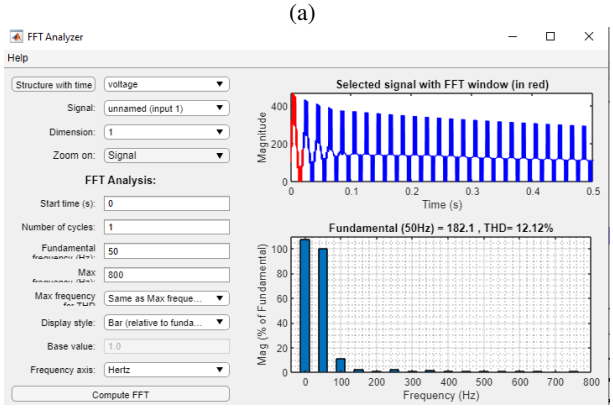

(b)

Fig. 17: Current harmonics when a five level inverter with NNFOPID and load torque 45N

simulation result is shown in Fig.18. By using NNFOPID controller with three five-level inverter during the no load condition the total voltage harmonic detection decreased from 12.12% to 6.82%.

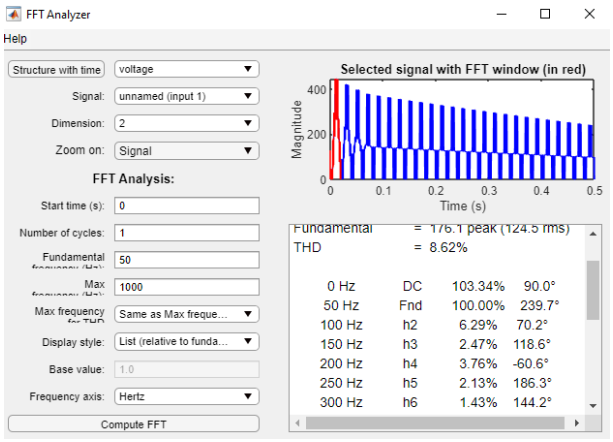

Fig. 18: Harmonics voltage with five level inverter and NN-FOPID with no load

The harmonics decreases for higher order level. As shown in Fig. 13, the load decreased from its rated value by 50%, harmonics reduce too.

VI. Conclusion

An IM speed drives inherently create harmonic currents as they take three-phase AC sinusoidal power and convert it to DC power as part of AC motor control. IGBT with freewheeling diodes, they all generate harmonics because they turn on and off, creating a current waveform that is not sinusoidal. Harmonic currents create voltage distortions on the power lines that feed the power converters. Poorly designed applications can result in the problem for power distribution equipment and other equipment attached to the same power distribution system. To overcome the problem, SVPWM vector control and five level three-phase inverter is designed. The NNFOPID controller is used to control the compensation process by controlling the discharging and charging process of the active filter. From the Matlab simulation result, current harmonics were improved from 68.87% to 2.79%.

References

[1] S. Nandagopal, H. K. Ravi, and L. N. Chokkalingam, "Harmonics study of five phase induction machine with different winding approaches for traction," in *2019 IEEE Transportation Electrification Conference (ITEC-India)*, IEEE, 2019, pp. 1–4.

[2] P. Ranga and M. Mittal, "Harmonic reduction in induction motor using harmonic injection method and passive filter: A comparison," in *2020 First IEEE International Conference on Measurement, Instrumentation, Control and Automation (ICMICA)*, IEEE, 2020, pp. 1–5.

[3] M. A. K. A. Biabani and S. M. Ali, "Control of induction motor drive using space vector pwm," in *2016 International Conference on Electrical, Electronics, and Optimization Techniques (ICEEOT)*, IEEE, 2016, pp. 3344–3351.

[4] C.-H. Hsu, "Fractional order pid control for reduction of vibration and noise on induction motor," *IEEE Transactions on Magnetics*, vol. 55, no. 11, pp. 1–7, 2019.

[5] J. Bača, D. Kouřil, P. Palacký, and J. Strossa, "Induction motor drive with field-oriented control and speed estimation using feedforward neural network," in *2020 21st International Scientific Conference on Electric Power Engineering (EPE)*, IEEE, 2020, pp. 1–6.

[6] W. T. Asfu, "Stator current-based model reference adaptive control for sensorless speed control of the induction motor," *Journal of control science and Engineering*, vol. 2020, pp. 1–17, 2020.

[7] U. Sengamalai, G. Anbazhagan, T. Thamizh Thentral, P. Vishnuram, T. Khurshaid, and S. Kamel, "Three phase induction motor drive: A systematic review on dynamic modeling, parameter estimation, and control schemes," *Energies*, vol. 15, no. 21, p. 8260, 2022.

[8] K. R. Sudharshana, V Muralidhara, A Ramachandran, and R Srinivasan, "Analysis of total harmonic distortion in 5-level inverter fed induction motor," in *2018 International Conference on Computing, Power and Communication Technologies (GUCON)*, IEEE, 2018, pp. 800–804.

[9] M Sujith and S Padma, "Optimization of harmonics with active power filter based on adaline neural network," *Microprocessors and Microsystems*, vol. 73, p. 102 976, 2020.

[10] A. S. Abdel-Khalik, S. Ahmed, and A. M. Massoud, "Steady-state mathematical modeling of a five-phase induction machine with a combined star/pentagon stator winding connection," *IEEE Transactions on Industrial Electronics*, vol. 63, no. 3, pp. 1331–1343, 2015.

[11] M Sujith and S Padma, "Optimization of harmonics with active power filter based on adaline neural network," *Microprocessors and Microsystems*, vol. 73, p. 102 976, 2020.

[12] T. Krenicky, Y. Nikitin, and P. Božek, "Model-based design of induction motor control system in matlab," *Applied Sciences*, vol. 12, no. 23, p. 11 957, 2022.

[13] N. Surasmi and G Shiny, "Harmonic mitigation in induction-motor drives using active filtering approach," in *2020 IEEE International Power and Renewable Energy Conference*, IEEE, 2020, pp. 1–6.

[14] Z. Ye, B. Wu, and N Zargari, "Modeling and simulation of induction motor with mechanical fault based on winding function method," in *2000 26th Annual Conference of the IEEE Industrial Electronics Society. IECON 2000. 2000 IEEE International Conference on Industrial Electronics, Control and Instrumentation. 21st Century Technologies*, IEEE, vol. 4, 2000, pp. 2334–2339.

[15] G. Qin, M. Liu, J. Zou, and X. Xin, "Vector control algorithm for electric vehicle ac induction motor based on improved variable gain pid controller," *mathematical problems in engineering*, vol. 2015, 2015.

[16] N. Djagarov, H. Milushev, M. Bonev, Z. Grozdev, and J. Djagarova, "Adaptive vector control of induction motor drives by optimal adaptive observer," in *2020 7th International Conference on Energy Efficiency and Agricultural Engineering (EE&AE)*, IEEE, 2020, pp. 1–5.

[17] I. Ferdiansyah, L. P. S. Raharja, D. S. Yanaratri, and E. Purwanto, "Design of pid controllers for speed control of three phase induction motor based on direct-axis current (id) coordinate using ifoc," in *2019 4th International Conference on Information Technology, Information Systems and Electrical Engineering (ICITISEE)*, IEEE, 2019, pp. 369–372.

[18] I. Ferdiansyah, M. R. Rusli, B. Praharsena, H. Toar, E. Purwanto, *et al.*, "Speed control of three phase induction motor using indirect field oriented control based on real-time control system," in *2018 10th International*

Conference on Information Technology and Electrical Engineering (ICITEE), IEEE, 2018, pp. 438–442.

[19] C.-H. Hsu, "Fractional order pid control for reduction of vibration and noise on induction motor," *IEEE Transactions on Magnetics*, vol. 55, no. 11, pp. 1–7, 2019.

[20] A. L. Saleh, B. A. Obaid, and A. A. Obed, "Motion control of linear induction motor based on optimal recurrent wavelet neural network-pid controller," *International Journal of Engineering & Technology*, vol. 7, no. 4, pp. 2028–2034, 2018.

[21] I. Ferdiansyah, M. R. Rusli, B. Praharsena, H. Toar, E. Purwanto, *et al.*, "Speed control of three phase induction motor using indirect field oriented control based on real-time control system," in *2018 10th International Conference on Information Technology and Electrical Engineering (ICITEE)*, IEEE, 2018, pp. 438–442.

[22] B. Amarapur, "Neural network based speed control of induction motor," in *2013 Nirma University International Conference on Engineering (NUiCONE)*, IEEE, 2013, pp. 1–6.

[23] J. Liceaga-Castro, L. Amezquita-Brooks, and E. Liceaga-Castro, "Induction motor current controller for field oriented control using individual channel design," in *2008 34th Annual Conference of IEEE Industrial Electronics*, IEEE, 2008, pp. 235–240.

[24] L. E. Venghi, F. Aguilera, P. M. de la Barrera, and C. H. De Angelo, "Design of discrete-time current controllers for induction motor drives based on an individual channel analysis approach," in *2019 Argentine Conference on Electronics (CAE)*, IEEE, 2019, pp. 70–75.

[25] O. Rodríguez-Abreo, J. Rodríguez-Reséndiz, C. Fuentes-Silva, R. Hernández-Alvarado, and M. D. C. P. T. Falcón, "Self-tuning neural network pid with dynamic response control," *IEEE Access*, vol. 9, pp. 65 206–65 215, 2021.

[26] H. Abu-Rub, A. Iqbal, and J. Guzinski, "Pyrighted m," 2012.